Research Journal of Recent Sciences ISSN 2277-2502
Vol. **15(3),** 8-15, July **(2026)** *Res. J. Recent Sci.*

Alkaline Desilication–Induced Matrix Densification and Rare Earth Element Retention in Coal Fly Ash

Vinod Kumar*, Akanksha Aggarwal, Amit Kulshershtha, Manish Kumar, Shanta Kumar, Raj Kumar Tripathi, Yashwant Kumar Saini and Shyam Manohar Gupta
NTPC Energy Technology Research Alliance (NETRA), Plot No. E-3, Ecotech-II, Udyog Vihar, Greater Noida -201306, Uttar Pradesh, India
vndkumar933@gmail.com

Available online at: www.isca.in, www.isca.me
Received 9th April 2026, revised 20th May 2026, accepted 25th June 2026

Abstract

Coal fly ash (CFA), an aluminosilicate-rich by-product obtained after coal combustion, is a potential secondary resource for rare earth elements (REEs). This study evaluates a matrix-engineering approach based on alkaline desilication–induced densification to restructure the host framework while retaining REEs in the solid phase. Magnetic separation followed by controlled treatment with 4 M NaOH (solid-to-liquid ratio 1:5) was applied to CFA from an Indian thermal power plant. Major oxides were analyzed by ED-XRF and 18 REEs were quantified using ICP–MS. Magnetic separation removed only 3.68% of the total mass, indicating limited association of REEs with strongly magnetic iron phases. Alkaline treatment achieved >92% silica removal, reducing SiO_2 from 58.55 wt.% to 4.41 wt.% and enriching Al_2O_3 to 85.00 wt.% in the bottom-settled fraction. The slurry stratified into density-driven layers, with the alumina-rich residue representing a densified structural phase. Despite extensive desilication, REEs remained predominantly in the solid phase. The abundance pattern (Ce > La > Nd > Y > Sc > Dy) was preserved across treated fractions, and critical elements such as Nd and Dy were retained in the densified residue. Observed decreases in ppm values reflect matrix mass redistribution rather than significant alkaline solubilization. The process is best described as alkaline desilication–induced matrix densification with stratified REE retention. This acid-minimizing strategy upgrades CFA into an alumina-enriched precursor suitable for downstream targeted REE recovery, supporting sustainable resource utilization.

Keywords: Coal Fly Ash; Rare Earth Elements; Alkaline Desilication; Matrix Densification; REE Retention; ICP-MS.

Introduction

The by-product of combustion of coal in the boiler of a coal-based power plant is collectively called coal ash which includes bottom ash (the course portion settling in furnace bottom) and fly ash (the lighter portion flying with the flue gas and collected by the electrostatic precipitators)[1]. Globally, hundreds of millions of tonnes of CFA are generated annually, and large stockpiles continue to accumulate, posing long-term environmental risks including groundwater contamination, air pollution, and land degradation[1,2]. While significant efforts have focused on the utilization of CFA in cement, construction materials, and geopolymers[3,4], comparatively fewer studies have investigated its systematic valorization as a rare earth resource, particularly through matrix-controlled processing approaches. Most existing investigations are based on laboratory-ash coal samples prepared for analytical purposes, rather than fly ash obtained from large- scale thermal power plant stockpiles, where phase composition and elemental distribution differ significantly[5,6].

Furthermore, the growing adoption of biomass co-firing in power plants has led to the generation of coal–biomass fly ashes with distinct physicochemical properties, often rendering them unsuitable for traditional applications such as cement and concrete[7,8]. These altered ash characteristics, however, may favour rare earth element (REEs) enrichment and nucleation under controlled processing conditions[8]. Therefore, systematic investigation of nucleation behaviour and phase evolution of the REEs present in fly ashes resulting from the combustion of coal or coal–biomass blends is essential to develop sustainable and alternative utilization pathways for these emerging waste streams[9].

Recovering REEs from CFA offers various benefits over traditional rare earth ore processing, particularly when recovery is guided by controlled nucleation mechanisms[9,10]. CFA is often enriched in heavy and critical REEs relative to light REEs, enhancing its strategic value for advanced technological applications[10]. As a combustion by product, CFA eliminates the need for additional mining, thereby significantly reducing extraction costs and environmental disturbance. Moreover, CFA generally contains lower concentrations of naturally occurring radio nuclides such as uranium and thorium compared to primary rare earth ores, simplifying downstream processing and waste management[10,11].

Although the potential of CFA as a promising rare earth resource has been discussed in the literature, most studies have focused on compositional assessments and geological

characteristics rather than on recovery mechanisms governed by nucleation behaviour[11]. The cumulative global demand for REEs and limitations in primary supply have intensified interest in alternative sources[22,23]. Reported average REE contents in lignite and bituminous coal fly ashes worldwide are approximately 378 and 469 ppm, respectively, with several deposits exhibiting significantly higher concentrations[11,12]. A mechanistic understanding of REEs nucleation and phase evolution during processing is therefore essential for developing selective, efficient, and environmentally sustainable recovery strategies from CFA[12].

REEs are commonly classified into critical and non-critical categories based on their supply risk, economic importance, nucleation and extraction challenges as listed in Table-1[13]. These elements are indispensable for modern technologies like advanced electronics, renewable energy systems, electric vehicles, permanent magnets, catalysts, and defence applications due to their unique luminescent, magnetic, and electrochemical properties[13,14]. In natural deposits, REEs typically coexist closely within mineral matrices, necessitating complex and multi-step separation and purification processes[15].

Table-1: Critical and Non-Critical REEs.

Category	REEs	Reason
Critical	Nd, Dy, Tb, Eu, Y, Sm, Pr, Gd	Complex leaching, solvent extraction, ion-exchange, rare ores
Non-Critical	Ce, La, Pm, Sc, Ho, Er, Tm, Yb, Lu	Easier leaching, more abundant, simpler separation

The strategic importance of REEs nucleation, extraction, and processing has become a national priority in many countries to ensure economic competitiveness and technological security[16]. In this context, developing a domestic supply chain through sustainable and alternative sources is critical[17]. CFA has emerged as a promising alternative, and integrating nucleation-driven processing methods offers a viable pathway for selective recovery. Controlled nucleation during alkaline treatment can enhance separation efficiency while reducing reliance on conventional acid-intensive extraction routes, thereby supporting environmentally responsible REE production[17,18].

Alkaline pre treatment and desilication was employed as a pretreatment strategy for the recovery of REEs from CFA under controlled nucleation conditions[18]. The present study introduces a matrix-engineering strategy termed alkaline desilication–induced densification under controlled nucleation conditions. Unlike conventional extraction-driven approaches, this method focuses on selective silica removal to densify the aluminosilicate framework while retaining REEs within a structurally transformed solid precursor. By employing magnetic pre-separation followed by 4M NaOH treatment at controlled solid–liquid ratios, this work investigates: The extent of silica removal and alumina enrichment, The redistribution and retention behaviour of 18 REEs during alkaline treatment, and The mechanistic implications of density-driven stratification in treated residues.

This approach aims to establish an acid-minimized, low-carbon pretreatment pathway that converts CFA from a bulk waste material into a structurally optimized precursor for downstream selective REE recovery. By integrating matrix densification with nucleation control, the study contributes to the advancement of sustainable rare earth extraction technologies and supports circular economy frameworks for coal-derived waste streams. The alkaline environment promotes partial dissolution of the amorphous silicon–aluminium framework present in CFA, thereby weakening the aluminosilicate structure without complete matrix destruction[19,20]. This controlled structural modification facilitates the release and redistribution of REEs into the alkaline medium, creating supersaturation conditions favourable for nucleation and selective phase formation[20].

Maintaining a solid-to-liquid ratio of 1:5 ensures sufficient reagent availability while minimizing excessive bulk dissolution and secondary waste generation. Variation in sodium hydroxide (NaOH) concentration allows systematic evaluation of dissolution kinetics, silicon extraction efficiency, and REEs nucleation behaviour[21,22]. Lower concentrations promote moderate structural disruption, whereas higher molarities enhance matrix breakdown and influence supersaturation levels, thereby directly affecting nucleation dynamics. This integrated approach enables optimization of alkaline treatment conditions to maximize REEs recovery while preserving process sustainability and minimizing environmental impact[23,24].To the best of our knowledge, this is the first study to examine alkaline desilication–induced structural densification as a strategy for retaining REEs within alumina-enriched residues derived from Indian CFA.

Materials and Methods

Raw Material Collection and Preparation: The CFA used in this study was collected from NTPC Thermal Power Station (NTPS) located in Uttar Pradesh, India. The ash sample was dried in hot air oven at 105°C for 24 h to remove moisture, then sieved to <75 μm to maximize the surface area for chemical reactions. At ambient temperature, the homogenized sample was stored in vacuum-sealed plastic bags before further treatment and analysis.

Chemicals and Reagents: The analytical-grade chemicals employed in the study included 65% nitric acid (HNO_3, Suprapur grade, Merck), 30% hydrochloric acid (HCl, Suprapur grade, Merck), 40% hydrofluoric acid (HF, AR grade, Rankem), and sodium hydroxide pellets (NaOH, Merck). Ultrapure deionized Type I water (resistivity ≥18.2 MΩ·cm) was delivered using an Elga Lab water purification system and used for all solution preparation and washing steps.

Pre-treatment of Coal Fly Ash: Magnetic Separation: Magnetic separation was conducted to remove iron-rich ferromagnetic phases, primarily magnetite (Fe_3O_4) and hematite (Fe_2O_3), which may interfere with subsequent alkaline dissolution and REE redistribution. Approximately 25g of dried CFA was spread as a thin layer (<5 mm thickness) on a non-magnetic surface. A hand-held neodymium bar magnet was passed repeatedly over the sample until no further magnetic particles were recovered. The procedure is illustrated in Figure-1. The magnetic fraction (MF) and non-magnetic fraction (NMF) were collected and weighed separately to determine mass distribution. The non-magnetic fraction was used for subsequent alkaline treatment to minimize iron-associated interference during desilication and nucleation processes.

Figure-1: Coal Fly Ash Treatment with Bar Magnet.

Alkaline Leaching and Controlled Nucleation: Alkaline treatment was performed to selectively dissolve silica and partially disrupt the aluminosilicate matrix, thereby inducing favourable super saturation conditions for REE redistribution and retention within the densified matrix. The iron-depleted residue (10g) was subjected to alkaline leaching with 4M NaOH solution at a solid-to-liquid ratio of 1:5 (g/mL). The temperature was maintained between 80 and 95°C for 2 to 4 hours under continuous stirring (300 rpm) using a magnetic stirrer to ensure uniform mixing and effective mass transfer. The alkaline environment promotes selective dissolution of amorphous SiO_2, partial breakdown of aluminosilicate frameworks, redistribution of REEs within the evolving matrix, and formation of supersaturated local environments conducive to nucleation. After completion of the reaction, the resulting slurry was vacuum filtered and washed with ultrapure water until a neutral pH was achieved to eradicate residual alkali.

The filtered solids were designated as REE-A, REE-B, and REE-C depending on the sequential washing step. The filtered solid residues are illustrated in Figure-2.

Analytical Instrumentation: Major elemental composition was determined using energy dispersive X-ray fluorescence (ED-XRF), while REE concentrations were quantified using inductively coupled plasma mass spectrometry (ICP-MS) following complete acid digestion.

EDXRF Analysis: Bulk chemical composition analysis of CFA for major and minor elements other than REEs was determined using EDXRF. The technique was employed to quantify oxide-forming elements such as aluminium (Al), silicon (Si), calcium (Ca), iron (Fe), potassium (K), magnesium (Mg), sodium (Na), and titanium (Ti). EDXRF analysis was selected due to its non-destructive nature, minimal sample preparation, and suitability for bulk compositional analysis of CFA. The results provided baseline compositional data to support alkaline leaching behaviour and nucleation-based REEs recovery. Instrument calibration was performed using certified reference materials. Analytical precision was maintained within ±2% relative standard deviation (RSD).

ICP-MS Analysis: For trace REEs quantification, complete acid digestion of solid samples was performed prior to ICP–MS using the method described by Raj *et al*[8]. The digested samples were analysed using ICP–MS operated in kinetic energy discrimination (KED) mode with > 99.99% pure argon and helium. The system was calibrated to detect concentrations as low as 0.01 ppm, with RF power at 1600 W and oxide formation limited to <2.5%. The instrumental parameters used for the quantification of REEs in CFA are listed in Table-2.

Prior to data acquisition, the operating conditions were optimized through a daily performance check using a multi-element tuning solution to achieve high analytical sensitivity. No correction equations were applied to any of the reported elemental analyses.

Results and Discussion

Baseline Composition and REE Inventory: The oxide composition of the as-received CFA, determined by ED-XRF, is presented in Figure-3. The material is predominantly composed of silica (58.55 wt.%) and alumina (27.74 wt.%), confirming its classification as a Class F aluminosilicate-rich ash[21]. The combined SiO_2 + Al_2O_3 content (~86 wt.%) indicates a stable glassy framework in which REEs are structurally entrapped within amorphous and crystalline phases. The structural encapsulation of REEs within this stable matrix explains the limited accessibility under conventional direct leaching conditions, thereby justifying the need for matrix-modification pretreatment.

Figure-2: Filtration procedure and residue for further analysis.

Table-2: Quantitative Parameters of ICP–MS employed[8].

Component/Parameter	Operating conditions
Spray chamber	Baffled glass cyclonic with AMS port
Nebulizer type	Meinhard Type CT Q+
Torch/Injector	Quartz with integrated 2.5mm id injector
RF power	1600 W
Plasma gas flow	15 L/ min
Auxiliary gas flow	1.20 L/ min
Nebulizer gas flow	1.02 L/ min
Collision gas flow	5 mL/ min

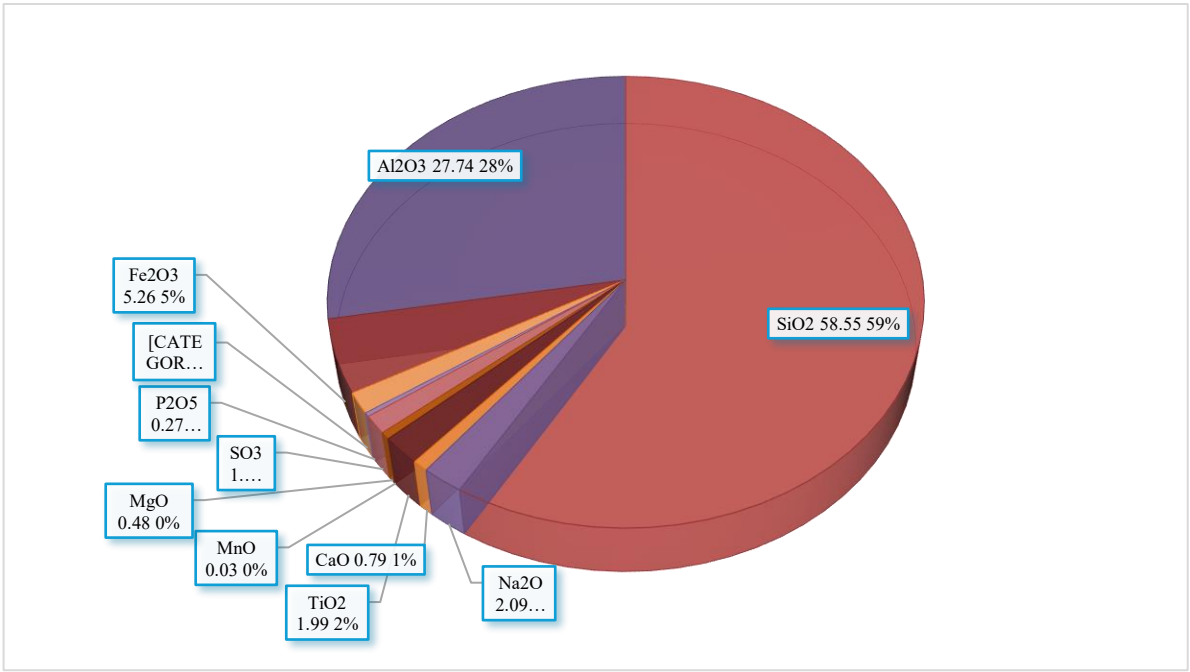

Figure-3: Composition of the Raw CFA with oxide concentration (wt%).

In the nucleated phases intended for REE recovery (Samples REE-A, B& C), the oxide distribution shifts dramatically. ICP-MS analysis identified 18 REEs in the raw ash, with Ce (149.20 ppm), La (76.83 ppm), Nd (54.29 ppm), and Y (46.20 ppm) as the most abundant species as shown in Table-3. ICP-MS analysis revealed a total REE concentration of 447.01 ppm in the raw CFA, consistent with reported global values (200–500 ppm)[20]. The abundance profile follows:

Ce > La > Nd > Y > Sc > Dy

This distribution reflects typical light-REE dominance in coal-derived materials, with measurable quantities of critical elements such as Nd and Dy. The total REE concentration is consistent with reported global averages for lignite and bituminous fly ashes[11,12], reinforcing the resource potential of the studied material. This baseline establishes both the structural rigidity of the aluminosilicate matrix and the initial REE inventory prior to matrix modification.

Effect of Magnetic Pre-Treatment: Magnetic separation was conducted to isolate iron-rich ferromagnetic particles prior to alkaline treatment. The initial mass of CFA processed was 25.00 g. Magnetic separation removed 3.68% of the total mass (Table-4), indicating that strongly magnetic iron-bearing phases (e.g., magnetite) constitute a minor fraction of the bulk material. The non-magnetic fraction accounted for 96.32% of the mass and retained the majority of REEs.

Table-3: The concentrations for key REEs in the raw ash and the solid residues (REE A, B & C) are summarized.

REE	Raw CFA (Avg. ppm)	REE Residue A (Avg. ppm)	REE Residue B (Avg. ppm)	REE Residue C (Avg. ppm)
Ce	149.20	113.82	112.39	101.16
Dy	8.84	6.79	6.67	6.18
Er	4.70	3.68	3.61	3.29
Eu	1.74	1.37	1.33	1.20
Gd	10.57	8.27	8.07	7.34
Ho	1.44	1.11	1.09	1.01
La	76.83	59.58	59.27	53.43
Lu	0.50	0.40	0.39	0.35
Nd	54.29	39.88	39.56	36.41
Pr	13.84	10.60	10.50	9.43
Sc	27.41	21.32	21.04	18.76
Sm	11.15	8.68	8.47	7.66
Tb	1.34	1.03	1.01	0.92
Th	28.62	18.63	18.26	16.20
Tm	0.55	0.43	0.42	0.38
U	6.44	3.30	3.06	2.67
Y	46.20	36.89	35.18	32.12
Yb	3.34	2.65	2.56	2.33
Total REE	447.01	338.43	332.89	300.85

Table-4: Mass Balance after Magnetic Separation.

Fraction	Mass (g)	Recovery (%)
Magnetic Fraction (MF)	0.92	3.68
Non-Magnetic Fraction (NMF)	24.08	96.32
Total	25.00	100.00

This observation suggests that REEs are not predominantly hosted within strongly magnetic iron phases. Instead, they are likely associated with aluminosilicate glass and weakly magnetic or non-magnetic mineral components. Therefore, magnetic separation primarily serves as matrix conditioning rather than a significant REE concentration step.By reducing iron-associated interference, this step improves alkali utilization efficiency during subsequent desilication.

Alkaline Desilication and Matrix Transformation: The alkaline treatment is specifically aimed at silica extraction. REE-A, B& C represent three stratified solid residues obtained after 4 M NaOH treatment and sequential washing: i. REE-A: top suspended layer, ii. REE-B: intermediate layer, iii. REE-C: bottom settled layer.

Oxide Redistribution Across Stratified Residues: The oxide composition (Table-5) demonstrates a pronounced compositional gradient: i. SiO_2 decreased from 58.55 wt.% (raw) to 4.41 wt.% (REE-C), ii. Al_2O_3 increased from 27.74 wt.% to 85.00 wt.% in REE-C.

Table-5: Compositional Gradient of Major Oxides across Slurry Layers after alkaline Treatment (wt.%).

Component	Concentration (wt.%)			
	Raw CFA	REE-A	REE-B	REE-C
Silicon Dioxide (SiO2)	58.55 ± 0.15	52.47 ± 0.18	51.12 ± 0.18	4.41 ± 0.59
Aluminium Oxide (Al2O3)	27.74 ± 0.11	26.49 ± 0.13	25.49 ± 0.13	85.00 ± 2.00
Iron Oxide (Fe2O3)	5.26 ± 0.02	7.02 ± 0.03	7.39 ± 0.03	0.85 ± 0.36
Sodium Oxide (Na2O)	2.09 ± 0.17	8.97 ± 0.27	10.56 ± 0.30	0.07 ± 0.21

This corresponds to92.4% silica removal, strong alumina enrichment, and significant structural densification. REE-A and REE-B remained silica-rich (~51–52 wt.% SiO_2), whereas REE-C represents a densified alumina-dominant residue. The progressive increase in Na_2O (up to ~10.5 wt.% in REE-B) reflects incorporation of sodium during desilication and confirms active alkaline participation in matrix restructuring.

This suggests that during alkaline treatment: i. Silica dissolution occurred throughout the slurry, implying NaOH acted as a desilication agent, breaking Si–O–Si bonds and forming soluble sodium silicate species. ii. Denser alumina-rich residual particles settled preferentially because the preferential dissolution of silica weakened the glassy matrix and facilitated internal restructuring of residual particles. iii. Less-reacted or silica-containing particles remained suspended longer. This layered separation reflects density-driven settling behaviour rather than sequential chemical transformation. Thus, REE-C represents a densified, structurally transformed fraction.

This data confirms strong desilication under alkaline conditions, resulting in matrix densification and alumina enrichment.

Mechanism of Selective Silica Dissolution: Under moderately alkalineconditions, amorphous silica reacts according to:

$$SiO_2 + 2NaOH \rightarrow Na_2SiO_3 + H_2O$$

Key mechanistic consequences include: i. Breakage of Si–O–Si bonds, ii. Formation of soluble sodium silicate, iii. Weakening of the glassy aluminosilicate matrix, iv. Increase in residual particle density.

As silica dissolves, alumina-rich skeletal structures persist. This leads to particle densification, density-driven settling, and formation of a bottom alumina-rich fraction (REE-C). Importantly, the observed stratification is therefore density-controlled, not sequential chemical transformation. In other words, as silica was removed, the residual particles became progressively enriched in alumina, increasing density and promoting gravitational settling. This confirms that alkaline treatment induces matrix densification rather than complete matrix destruction.

Rare Earth Element Behaviour During Matrix Densification: The REE concentration trend across fractions via ICP-MS analysis (Table-3) shows:

Raw CFA > REE-A ≈ REE-B > REE-C (in ppm)

There is a consistent reduction in the absolute ppm values of REEs from the raw CFA to the final REE Residue C. At first glance, the decrease in absolute ppm values in REE-C might suggest REE loss. However, interpretation must consider matrix transformation and mass redistribution. This correlates with the EDXRF data showing the concentration of alumina (Al_2O_3) in the final residue, which suggests that while the REEs are retained in the nucleated phases, the overall mass balance shifts as bulk oxides are removed.

Despite extreme desilication (>90% silica removal), REEs remained largely associated with the solid phase. Notably, Ce remained dominant (149 → 101 ppm), Nd retained significant concentration (54 → 36 ppm), Dy persisted at measurable levels (8.84 → 6.18 ppm) and Trace HREEs (Tm, Lu) were consistently detected. These results suggest that: i. Limited REE solubility under 4 M NaOH conditions. ii. Structural entrapment within alumina-rich residues. iii. Absence of extensive alkaline mobilization.

Thus, this data indicates that REEs are primarily hosted within the aluminosilicate matrix rather than strongly magnetic iron phases because the magnetic fraction is only 3.68% of total mass, Fe-rich phases were minor, and REEs persist in alumina-rich residue.

Implications for Process Design: The combined magnetic and alkaline results indicate minimal hosting in strongly magnetic phases, strong association with aluminosilicate matrix and persistence in densified alumina-rich residue. This supports the hypothesis that REEs are structurally bound within the amorphous aluminosilicate glass, residual alumina frameworks and possibly nano-scale dispersed phases resistant to alkaline attack.

The transformation from silica-rich to alumina-rich matrix does not liberate REEs into solution but instead concentrates them within a structurally modified solid precursor.

The process can be summarized in three stages: i. Matrix Conditioning Magnetic removal of iron-rich phases. ii. Selective Desilication Dissolution of SiO_2 → formation of Na_2SiO_3. iii. Density-Driven Stratification Alumina-rich skeletal particles densify and settle, retaining REEs.

This mechanism differs fundamentally from extraction-driven approaches. Instead of mobilizing REEs into aggressive leachates, the method restructures the matrix, removes bulk silica and generates a densified REE-bearing precursor. Therefore, it is best described as 'Alkaline desilication–induced matrix densification with stratified REE retention'.

Limitations and Implications for Process Optimization: While silica removal, alumina encrichment and solid-phase REE retention were clearly demonstrated, a quantitative REE mass balance between solid and liquid phases was not established in the present study. Future work will include direct measurement of REEs in alkaline leachates to determine precise retention efficiency.

Additionally, phase identification techniques such as XRD and SEM-EDS are required to confirm whether new REE-bearing phases form during desilication. While laboratory-scale recovery efficiencies appear promising, process scalability and reagent consumption remain key determinants of techno-economic viability.

Conclusion

This study demonstrates that Indian CFA can be structurally transformed through alkaline desilication while retaining REEs within the solid phase. Magnetic pre-treatment removed only 3.68% of the total mass, confirming that strongly magnetic iron oxides constitute a minor fraction and are not the dominant REE hosts. The primary REE inventory is therefore associated with the aluminosilicate matrix rather than ferromagnetic phases.

Treatment with 4 M NaOH induced selective silica dissolution, reducing SiO_2 from 58.55 wt.% to 4.41 wt.% (>92% removal) and enriching Al_2O_3 from 27.74 wt.% to 85.00 wt.% in the bottom-settled fraction (REE-C).

This compositional shift confirms extensive desilication and matrix densification. The stratification of residues (REE-A, REE-B, REE-C) is interpreted as a density-driven process resulting from progressive silica removal and structural restructuring of alumina-rich skeletal frameworks.

ICP–MS analysis showed that, despite significant bulk matrix transformation, REEs remained predominantly associated with the solid phase. The abundance trend (Ce > La > Nd > Y > Sc > Dy) persisted across all treated fractions, and critical elements such as Nd and Dy remained detectable in the densified alumina-rich residue. Although absolute ppm values decreased from raw CFA to REE-C, this reflects matrix mass redistribution rather than extensive alkaline solubilization.

The results indicate limited REE mobility under moderately alkaline conditions and suggest structural retention within the transformed aluminosilicate framework.

The process is therefore best described as alkaline desilication–induced matrix densification with stratified REE retention. Rather than directly dissolving REEs, the treatment restructures the aluminosilicate framework and produces a pre-concentrated solid suitable for targeted downstream extraction.

This approach provides a potentially low-carbon, acid-minimizing strategy for valorizing CFA as a secondary rare earth resource and supports the development of sustainable domestic critical mineral supply chains.

Acknowledgement

The authors sincerely acknowledge Shri S. Shaswattam, ED-NETRA, for his continuous support and valuable guidance in promoting the exploration of advanced condition monitoring techniques for the sustainable development of the power sector.

The authors also express their gratitude to Smt. G.D. Vani and Dr. A Lakshman Kumar for her dedicated laboratory assistance during the execution of the present study.

References

1. Stoy, L., Diaz, V. & Huang, C. H. (2021). Preferential recovery of rare-earth elements from coal fly ash using a recyclable ionic liquid. *Environmental Science & Technology*, 55(13), 9209–9220.

2. Liu, P., Zhao, S., Xie, N., Yang, L., Wang, Q., Wen, Y., Chen, H., & Tang, Y. (2023). Green approach for rare earth element (REE) recovery from coal fly ash. *Environmental Science & Technology*, 57(13), 5414–5423.

3. Kim, G. M., Park, S., Choi, J., Park, S., & Kim, J. (2024). Effects of alkaline extraction on behavior of rare earth elements in coal ashes. *Environmental Science and Pollution Research*, 31(54), 63210-63224.

4. Zhang, W., Noble, A., Yang, X., & Honaker, R. (2020). A comprehensive review of rare earth elements recovery from coal-related materials. *Minerals*, 10(5), 451.

5. Tian, X., Guo, Z., Zhu, D., Pan, J., Yang, C. & Li, S. (2025). Recovery of valuable elements from coal fly ash: A review. *Environmental Research*, 282, 121928.

6. Franus, W., Wiatros-Motyka, M. M., & Wdowin, M. (2015). Coal fly ash as a resource for rare earth elements. *Environmental Science and Pollution Research*, 22, 9464–9474.

7. Ajayi, L. O., Lejeune, B., Struppe, J., Guo, J., & Daramola, D. A. (2025). Alkali treatment implications for microwave-assisted rare earth elements extraction from coal mine tailings. *Environmental Science & Technology*, 59, 25044–25055.

8. Tripathi, R. K., Saini, R. K., Aggarwal, A., Kumar, A. L., Pranay. & Das, A. K. (2025). A case study for assessing coal fly ash in NTPC power stations as a potential source of rare earth elements. *International Journal of Engineering Research & Technology*, 14(4).

9. Pan, J., Hassas, B. V., Rezaee, M., Zhou, C., & Pisupati, S. V. (2020). Recovery of rare earth elements from coal fly ash through sequential chemical roasting, water leaching, and acid leaching processes. *Journal of Cleaner Production*, 284, 124725.

10. Bisen, S. V., Sharma, S., & Chattopadhyay, S. (2025). Rare earth elements occurrences in coal fly ash and methods of extraction: A review. *Journal of the Geological Society of India*, 101(5), 581–590.

11. 11.Thomas, B. S., Dimitriadis, P., Kundu, C., Vuppaladadiyam, S. S. V., & Bhattacharya, S. (2024). Extraction and separation of rare earth elements from coal and coal fly ash: A review on engineering advancements. *Journal of Environmental Chemical Engineering*, 12(3), 112769.

12. Tajayani, I. D., Sutijan, S., & Petrus, H. T. B. M. (2023). Precipitation of rare earth element from Indonesian coal fly ash using sodium sulphate. *Materials Science Forum*, 1093, 105–110.

13. Kim, G. M., Park, S., Choi, J., Park, S., & Kim, J. (2024). Effects of alkaline extraction on behavior of rare earth elements in coal ashes. *Environmental Science and Pollution Research*, 31(54), 63210–63224.

14. Zhang, L., Chen, H., Pan, J., Yang, F., Long, X., Yang, Y., & Zhou, C. (2025). Rare earth elements recovery and mechanisms from coal fly ash by column leaching using citric acid. *Separation and Purification Technology*, 362, 128471.

15. Wen, Z., Zhou, C., Pan, J., Cao, S., Hu, T., & Ji, W. (2020). Recovery of rare-earth elements from coal fly ash via optimized leaching. *Journal of Environmental Management,* 270, 110912.

16. Zhang, W., Noble, A., Yang, X., & Honaker, R. Q. (2020). A comprehensive review of rare earth elements recovery from coal-related materials. *Minerals*, 10(5), 451.

17. Tian, X., Guo, Z., Zhu, D., Pan, J., Yang, C., & Li, S. (2025). Recovery of valuable elements from coal fly ash: A review. *Environmental Research*, 282, 121928.

18. Franus, W., Wiatros-Motyka, M. M., & Wdowin, M. (2015). Coal fly ash as a resource for rare earth elements. *Environmental Science and Pollution Research*, 22(12), 9464–9474.

19. Saquib, M. F. U. R., Ameer, S. K., Munjial, P., & Aly, O. (2026). Sustainability assessment of hydrogen fuel cell vehicles versus fossil fuel vehicles: A Canadian perspective. 15(1), 11–15.

20. Aggarwal, A., Tripathi, R. K., Kumar, A. L., Sharma, P., & Das, A. K. (2025). Harnessing Indian coal fly ashes for rare earth elements recovery. NTPC Transactions on Energy Research (NTER 2025) (pp. 221–235).

21. American Society for Testing and Materials. (2008). *Standard specification for coal fly ash and raw or calcined natural pozzolan for use in concrete*. ASTM International.

22. Gambogi, J. (2020). Mineral commodity summaries: Rare earths. *US Geological Survey, Washington, DC https://www. usgs. gov/centers/nmic/rare-earths-statistics-and-information. Accessed*, *14*.

23. Together, S. S. (2013). International Energy Agency. *International Energy Agency: Paris, France*.

24. Hussain, Z., Dwivedi, D., & Kwon, I. (2024). Recovery of rare earth elements from low-grade coal fly ash using recyclable biosorbents. *Frontiers in Bioengineering and Biotechnology*, 12, 1385845.